AGU PUBLICATIONS

Paleoceanography

RESEARCH ARTICLE
10.1002/2015PA002880

Key Points:
- We present a 150 year Kuroshio transport variation using new coral $\delta^{15}N$ proxy
- Our coral record suggests the acceleration of Kuroshio intensity through the twentieth century
- We demonstrate the relationships between Kuroshio evolution and ENSO-PDO states

Supporting Information:
- Supporting Information S1

Correspondence to:
A. Yamazaki,
zaki@mail.sci.hokudai.ac.jp

Citation:
Yamazaki, A., T. Watanabe, U. Tsunogai, F. Iwase, and H. Yamano (2016), A 150-year variation of the Kuroshio transport inferred from coral nitrogen isotope signature, *Paleoceanography*, *31*, 838–846, doi:10.1002/2015PA002880.

Received 12 SEP 2015
Accepted 30 MAY 2016
Accepted article online 3 JUN 2016
Published online 27 JUN 2016

A 150-year variation of the Kuroshio transport inferred from coral nitrogen isotope signature

Atsuko Yamazaki[1,2,3], Tsuyoshi Watanabe[1,2], Urumu Tsunogai[4], Fumihito Iwase[5,6], and Hiroya Yamano[7]

[1]Faculty of Science, Hokkaido University, Sapporo, Japan, [2]KIKAI Institute for Coral Reef Sciences, Kikai town, Japan, [3]Atmosphere and Ocean Research Institute, The University of Tokyo, Kashiwa, Japan, [4]Graduate School of Environmental Studies, Nagoya University, Chikusa-ku, Japan, [5]Biological Institute on Kuroshio, Kuroshio Biological Research Foundation, Otsuki, Japan, [6]Shikoku Marine Life Laboratory, Otsuki, Japan, [7]Center for Environmental Biology and Ecosystem Studies, National Institute for Environmental Studies, Tsukuba, Japan

Abstract The Kuroshio Current is a major global ocean current that drives the physical ocean-atmosphere system with heat transport from tropical to temperate zones in the North Pacific Ocean. We reconstructed the variability of the Kuroshio transport over the past 150 years using coral skeletal nitrogen isotopic composition ($\delta^{15}N_{coral}$). A 150 year $\delta^{15}N_{coral}$ record (1859–2008 A.D.) is 4 times the length of the observational record (1971 to present) and could provide a direct comparison with global climate change, such as the Pacific Decadal Oscillation (PDO) index and El-Niño–Southern Oscillation (ENSO), through recent global warming. Coral cores from *Porites* were collected from Tatsukushi Bay in 2008 on the Pacific coast of Japan, which is located on the northern front of the Kuroshio Current. $\delta^{15}N_{coral}$ was used as a proxy to record the $\delta^{15}N$ of nitrate ($\delta^{15}N_{nitrate}$) controlled by the upwelling of subtropical subsurface water ($\delta^{15}N_{nitrate}$; ~ +2 − +3‰), and $\delta^{15}N_{coral}$ was negatively correlated with observations of the Kuroshio transport ($R = -0.69$, $P < 0.001$) and the 2 year lagged PDO index ($R = -0.63$, $P < 0.005$) from 1972 to 2007. The 150 year record of $\delta^{15}N_{coral}$ suggested that the Kuroshio transport varied with ~25 year cycle, and the amplitude became more stable, and the volume was intensified through the twentieth century. The Kuroshio transport was intensified by the La Niña state in the early 1900s and by the El Niño-PDO state after the 1920s. Our results suggested that the Kuroshio transport was influenced by the combined climate modes of ENSO and PDO during the last century.

1. Introduction

The atmosphere-ocean interaction is particularly strong over western boundary currents and directly influences global climate variability. The Kuroshio Current is located on the western ridge of subtropical gyre in north western Pacific. The El-Niño–Southern Oscillation (ENSO) and the Pacific Decadal Oscillation (PDO) play a key role in the climate variability of the subtropical gyre and the behavior of the Kuroshio Current [*Hu et al.*, 2015; *Kashino et al.*, 2009; *Qiu*, 2003]. The circulation of ENSO signals into midlatitudes through the Kuroshio Current has been reported by partial ocean physical data in the latter part of the twentieth century [*Qiu and Lukas*, 1996; *Yamagata et al.*, 1985]. The Aleutian Low is intensified by a positive PDO and strengthens the Kuroshio extension jet [*Qiu and Chen*, 2010], which spins up the subtropical gyre [*Hanawa and Kamada*, 2001], upstream of the Kuroshio Current. However, the variations of the past Kuroshio Current have not been well understood, as the observation data are limited to 40 years. Although sea surface temperature (SST) reconstructions from sediment cores suggested that the Kuroshio axis has fluctuated with the North Pacific climate variability on millennial time scales [e.g., *Sawada and Handa*, 1998; *Ujiié et al.*, 2003], there is no record of Kuroshio variability on a comparative time scale with a decadal climate mode such as ENSO and the PDO.

Coral skeletons have been widely used as a high-resolution paleo-environmental recorder at decadal to millennial time scales in different windows of geological time [e.g., *Cobb et al.*, 2003; *Watanabe et al.*, 2011]. The heat and water transport of the Kuroshio Current supports the tropical reef corals thriving in the temperate areas along the Pacific coast of Japan. Conventional geochemical approaches using coral Sr/Ca and $\delta^{18}O$ can deduce SST and salinity changes, which are also associated with the high saline and warm Kuroshio Current. However, additional factors such as local precipitation, air temperature changes, or coral growth effects may also influence coral geochemical proxies.

The western boundary currents transport not only heat northward but also nutrients to the surface ocean along the current axis, which is described as the "nutrient stream" in the North Atlantic [*Pelegrí et al.*, 1996].

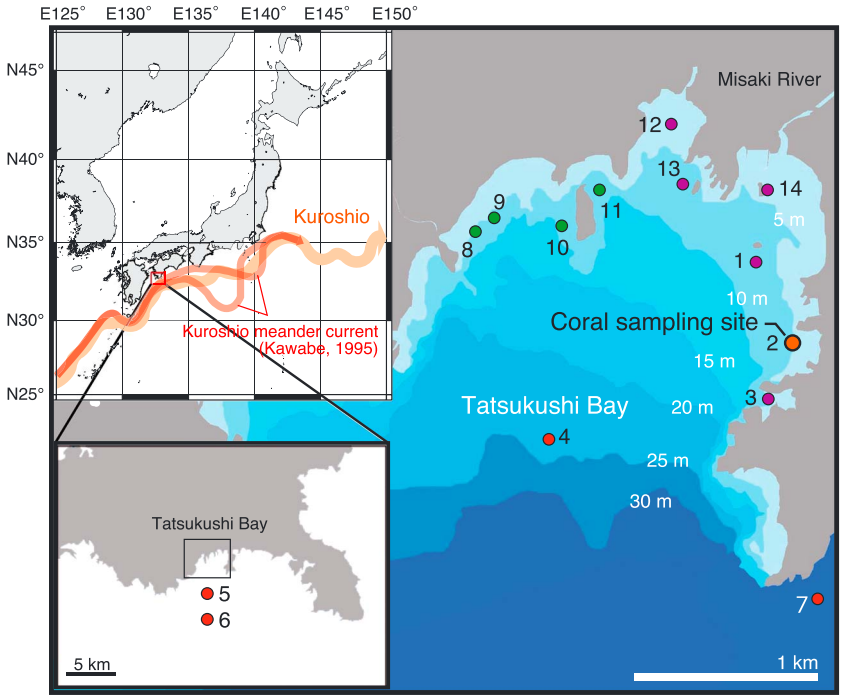

Figure 1. Coral core and water sampling sites in Tatsukushi Bay. The circle colors of each sites are corresponded with Figure 2. The location of the Kuroshio axis on the date of water sampling, 25 March 2010 (Japan Coast Guard, 2010) (orange arrow). The major locations of Kuroshio meander current from Kawabe (1995) (red arrows). The color-filled circles for each sites are indicated and repeated in Figure 2.

This dynamic system also influences marine production and ecosystems in the Northern Hemisphere. The upwelling along the Kuroshio path and extension areas is caused by the turbulence on the northern ridge of the Kuroshio axis [*Nagai et al.*, 2012; *Kaneko et al.*, 2012]. The turbulence is enhanced by frontogenesis and the associated secondary ageostrophic circulation, in addition to the symmetric instability between warm and cold water mass encountered at the Kuroshio front [*D'Asaro et al.*, 2011; *Nagai et al.*, 2009, 2012] and the interaction between the Kuroshio jet and internal waves [*Rainville and Pinkel*, 2004]. The larger gradient of water density with the larger volume of Kuroshio enhances the turbulent mixing. The nitrate supply along the Kuroshio axis has been observed from the East China Sea to the Pacific coast of Japan [*Kaneko et al.*, 2013; *Guo et al.*, 2013]. $\delta^{15}N_{nitrate}$ in the subsurface water of the north Pacific subtropical gyre is +2–+3‰ [*Liu et al.*, 1996; *Casciotti et al.*, 2008]. $\delta^{15}N_{nitrate}$ in the surface water has larger values than that in the subsurface due to the isotope fractionation caused by the nitrate consumption by primary producers. The mixing at the Kuroshio front supplies lower $\delta^{15}N_{nitrate}$ to the surface. Our use of $\delta^{15}N_{coral}$ has been recently established as a marker of the isotopic composition of oceanic nitrate that is assimilated by coral-symbiotic algae [*Yamazaki et al.*, 2011], which are preserved over geological time [*Muscatine et al.*, 2005; *Yamazaki et al.*, 2013]. $\delta^{15}N_{coral}$ used as a nutrient proxy could directly reveal important aspects of the history of the Kuroshio Current. Therefore, we demonstrate the variability of the Kuroshio transport over the past 150 years using a novel approach of $\delta^{15}N_{coral}$ related to nutrient dynamics on the Kuroshio front.

2. Materials and Methods

2.1. Coral Core Samples

Tatsukushi Bay, Kochi, Japan, is on the northern ridge of the Kuroshio Current and before the beginning of the meander current (Figure 1). On 13 October 2008, we drilled coral cores (ϕ6.4 cm) from a 1.5 m high live *Porites lutea* colony at a 3 m depth in Tatsukushi Bay (N32°46′38″, E132°52′13″), which is on the northern habitable limit of a long-living *Porites* colony (Figure 1). To minimize the chronological uncertainty, three coral cores were drilled side by side from the top of the continuous growth lines of the same coral colony. The coral cores were cut into 5 mm thick slabs. Clear annual bands are expressed in X-radiographs

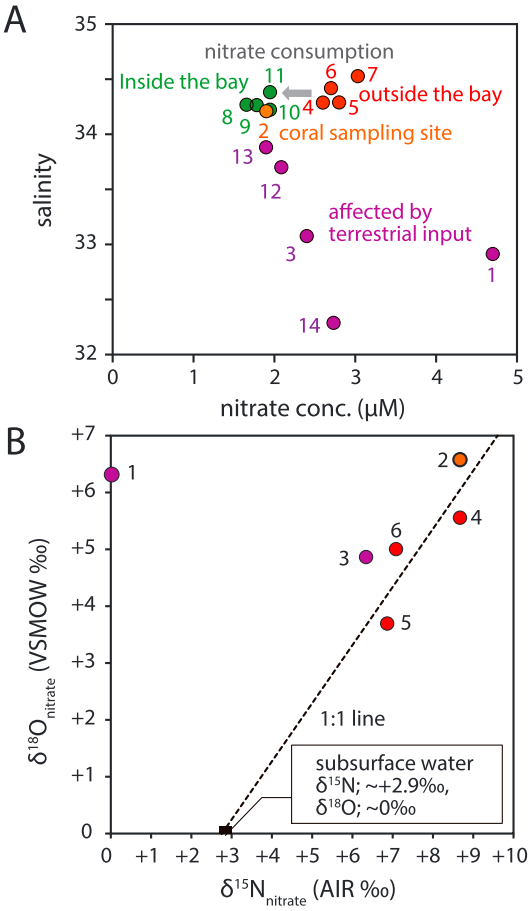

Figure 2. (a) Crossplot of nitrate concentrations and salinity in seawater samples in Tatsukushi Bay. The color-filled circles indicate each water sampling site and are repeated in Figure 2. Seawater affected by terrestrial water has lower salinity (purple circles). Seawater samples from inside the bay (green circles), including the coral sampling site (orange circle), have lower nitrate concentrations than seawater samples from outside (red circles). (b) Crossplot of $\delta^{15}N_{nitrate}$ and $\delta^{18}O_{nitrate}$ in seawater samples from st. 1–6. The nitrate from st. 1 has a different tendency than the others, which suggests that the nitrate at st. 1 might originate from terrestrial input. The dotted line (1:1 line) represents the hypothetical fractionation line for $\delta^{15}N$ and $\delta^{18}O$ resulting from nitrate assimilation. The nitrate isotope composition of upwelling water is expected to be ~ +2.3‰ for $\delta^{15}N$ and ~0‰ for $\delta^{18}O$.

(Figure S1 in the supporting information). A total of 216 annual bands were counted across the three cores, and analytical lines through 150 years were determined (Figure S1), excluding the bottom cores where dark and discontinuous annual bands were possibly altered by diagenesis (dissolution).

2.2. Age Model

The age model of the coral specimens was determined by comparing the couples of low- and high-density bands and the seasonal variation of coral $\delta^{18}O_{carbonate}$ (Figure S1). The variation in coral density was depicted by grey scale values of the X-radiographs using ImageJ 1.46 software (W. Rasband, the Research Services Branch, National Institute of Mental Health, Bethesda, Maryland, USA). Counting annual bands in former years (1792–1925) might cause an uncertainty of ~ ±2 years. The subsequent ages were determined by the comparison of the seasonality of $\delta^{18}O_{carbonate}$ with coral annual bands coupled with high-density (winter) and low-density (summer) bands [*Yamazaki et al.*, 2009]. $\delta^{18}O_{carbonate}$ records suggested that the growth rate of Tatsukushi coral was very slow and/or stopped under 18°C for 2–3 months a year, from January to March. Annual $\delta^{15}N_{coral}$ values were slightly biased toward the summer, when the Kuroshio transport is greater than in the winter (average summer (July–August) Kuroshio transport: $37.5 \times 10^6\ m^3\ s^{-1}$, average winter (January–February) Kuroshio transport: $31.4 \times 10^6\ m^3\ s^{-1}$ during 1972–2013 [*Japan Meteorological Agency*, 2013a, 2013b]).

2.3. Nitrogen Isotope Analysis

Subsampling was performed at 3 mm wide by 5 mm thick by 3 mm intervals at a subannual to annual resolution along the maximum growth axis to obtain 30–40 mg of coral powder. To remove the extra organic matter in the coral powder, the subsampled powder was treated with NaOH (2N, 60°C) for 3 h and rinsed using Milli-Q water [*Yamazaki et al.*, 2013]. A nitrogen isotope analysis of the dried powder samples was performed based on chemical conversion methods [*Yamazaki et al.*, 2011]. This method involves oxidation/reduction methods such as the oxidation of organic nitrogen to nitrate using persulphate [*Knapp and Sigman*, 2005; *Tsunogai et al.*, 2008, 2010], reduction of nitrate to nitrite using spongy cadmium, and further reduction of nitrite to nitrous oxide using sodium azide. Wet conditions were maintained throughout the chemical treatments to avoid the evaporation of dissolved organic nitrogen, which would affect the $\delta^{15}N$ values obtained after the re-drying process after acid treatment and to recover $\delta^{15}N$ in coral skeletons without isotope fractionation.

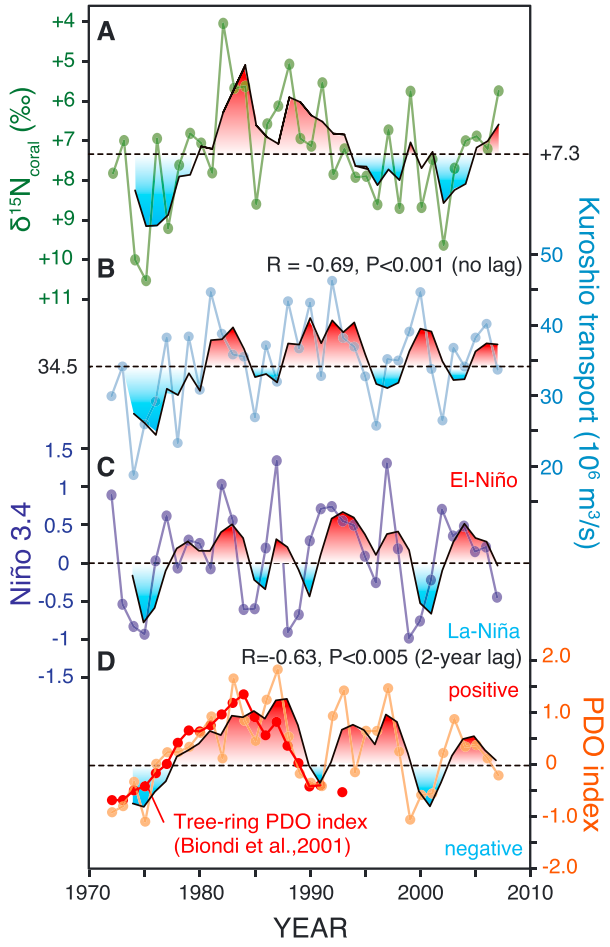

Figure 3. The annual resolution of (a) the $\delta^{15}N_{coral}$ time series during 1972–2007 is shown in comparison with (b) the Kuroshio transport at the 137°E line (Japan Meteorological Agency), (c) Nino3.4, and the (d) PDO index, each with a 3 year running mean (black). The *y* axis of $\delta^{15}N_{coral}$ (Figure 3a) is inverted. The Kuroshio transport data (Figure 3b) are from the Japan Meteorological Agency. The color shades and the arrow suggest lower (red) and higher (blue) anomalies from average values of $\delta^{15}N_{coral}$ (+7.3‰) and higher (red) and lower (blue) anomalies from the Kuroshio transport (34.5×10^6 m^3/s), Nino 3.4, and the PDO index. The correlation coefficients are −0.69 (R, $P < 0.001$) between $\delta^{15}N_{coral}$ and the Kuroshio transport and −0.63 (R, $P < 0.005$) between $\delta^{15}N_{coral}$ and the 2 year lagged PDO index.

Organic nitrogen in the coral skeletons was first oxidized to NO_3^- using persulphate under alkaline conditions. The coral skeletal powder (28 mg) was decalcified with 0.6 mL of 1N HCl in 30 mL Teflon bottles for 2 h. Then, followed by adding 0.4 mL of deionized water (DIW) and 50 μL of oxidizing reagent (peroxodisulphate [*Tsunogai et al.*, 2008]). The Teflon bottles were capped tightly with Teflon screw caps and autoclaved for 1 h at 121°C. After the samples were cooled for 8 h, needle crystals of $CaSO_4$ were deposited. A 1 mL volume of the sample solution, excluding the $CaSO_4$ crystals, and 9 mL of DIW were pipetted into 10 mL vials with butyl rubber caps. We used random two coral powder samples to add internal standards, including L-alanine ($\delta^{15}N = +1.78 \pm 0.06$‰AIR), L-histidine ($\delta^{15}N = -7.96 \pm 0.05$‰AIR), and tuna flakes ($\delta^{15}N = +12.55 \pm 0.06$‰AIR). Organic nitrogen standards diluted with DIW (400 μM-N) were oxidized to NO_3^- using the same methods. The internal standard samples contained the organic material of the coral skeletons (1 mL), 400 μM-N (1 mL), and 8 mL of DIW in 10 mL vials. Next, NO_3^- was reduced to NO_2^- by adding 0.5 g of spongy cadmium to each vial, followed by 0.3 g of NaCl and 0.1 mL of a 1 M $NaHCO_3$ solution to yield a final pH of approximately 8.5. The samples were then shaken for 5 h on a horizontal shaker at a rate of 2 cycles/s. Subsequently, NO_2^- was reduced to N_2O using sodium azide. Then, 10 mL of the samples was decanted into a clean 20 mL vial and capped tightly with a butyl rubber cap. After purging with helium to evacuate the air from the headspace and the sample solution for 2 min, 0.4 mL of azide/acetic acid buffer was added to each vial via a syringe, and the mixture was shaken. After 2 h, the solution was made basic by adding 0.2 mL of 8 M NaOH with a syringe and shaking to prevent residual HN_3 from escaping into the laboratory during the subsequent isotopic analysis. These chemical treatments were performed under wet conditions to prevent the evaporation of dissolved organic nitrogen, which would affect the $\delta^{15}N$ values obtained after the re-drying process after acid treatment and to recover all of the nitrogen in the skeletons.

The stable isotopic N_2O composition was determined using our continuous-flow isotope ratio mass spectrometry (CF-IRMS) system [*Tsunogai et al.*, 2008; *Konno et al.*, 2010; *Hirota et al.*, 2010], which consists of an initial helium purge and trap line, a gas chromatograph (Agilent 6890), and a Finnigan MAT 252 (Thermo Fisher Scientific, Waltham, MA, USA) with a modified Combustion III interface. $\delta^{15}N$ values were determined relative to $\delta^{15}N$ of air. The standard deviation of the coral sample measurements was less than 0.2‰ (σ, $n = 4$) [*Yamazaki et al.*, 2013].

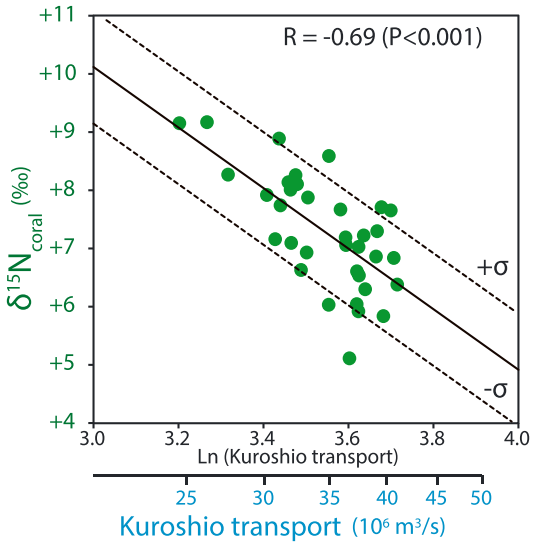

Figure 4. The correlation between the 3 year running means of $\delta^{15}N_{coral}$ and the logarithm of Kuroshio transport ($R = -0.69$). The P value ($P < 0.001$) was estimated by a Monte Carlo simulation with a thousand surrogate time series, using a phase randomization technique [*Kaplan and Glass*, 1995]. In this method, absolute Fourier amplitudes (square root of spectra) for the physical climate data such as Kuroshio transport time series were estimated, and then 1000 surrogate time series are generated by an inverse Fourier transform with the observed Fourier amplitudes and randomized phases. Surrogate correlation coefficients are estimated between the physical climate time series and $\delta^{15}N_{coral}$ time series. The relative position of the absolute value of the observed correlation coefficients in the sorted absolute values of the surrogate correlation coefficients gives the level of confidence for the observed correlation coefficient. This method takes into account the influences of the intrinsic serial correlation of respective time series. The second *x* axis shows raw Kuroshio transport value.

2.4. Seawater Analysis

Seawater samples were collected on 25 March 2010. One liter high-density polyethylene bottles were used for the water sampling. Seawater samples for the salinity analysis were decanted in 100 mL glass vials then capped tightly with butyl rubber caps and aluminum seals. For nitrate concentrations and the isotope analysis, seawater samples were filtered through precombusted 2.5 cm Whatman GF/F filters and refrigerated in 250 mL PPCO bottles until the analysis. The measurement of salinity was performed using an AUTOSAL Salinometer 8400B (Guildline Instrument) installed at the Geological Survey of Hokkaido, Japan. The sample NO_3^- was chemically converted to N_2O using same methods of coral skeletons [*Yamazaki et al.*, 2011]. The analyses of nitrate concentrations and nitrogen ($\delta^{15}N_{nitrate}$) and oxygen ($\delta^{18}O_{nitrate}$) isotopes were performed using an automated analytical system with continuous-flow isotope ratio mass spectrometry (CF-IRMS).

3. Results and Discussions

3.1. Nitrate Source of Tatsukushi Bay

Nitrate sources for Tatsukushi Bay are terrestrial input and seawater from the offshore. Salinity in the seawater samples from the coral sampling site was 34.223, which is most likely unaffected by river water and terrestrial input (Figure 2a). Nitrate concentrations outside of Tatsukushi Bay were ~1 μM higher than inside, which suggests that the nitrate source is outside the bay and that nitrate is consumed in the bay (Figure 2a). The $\delta^{15}N_{nitrate}$ and $\delta^{18}O_{nitrate}$ in the seawater from Tatsukushi Bay demonstrated that nitrate in the seawater at the coral sampling site was supplied from offshore and that $\delta^{15}N_{nitrate}$ increased through the nitrate assimilation by primary producers (Figure 2b).

3.2. The Recent 36 Year Variation of $\delta^{15}N_{coral}$

The recent 36-year (1972–2007) record of $\delta^{15}N_{coral}$ is compared to the volume of the Kuroshio transport at the N 137° line, estimated using hydrological observation data [*Japan meteorological Agency*, 2013a, 2013b], the NIÑO3.4 SST index [*Earth System Research Laboratory, NOAA*, 2013] for ENSO variability, and the PDO index [*Mantua et al.*, 1997] with the tree ring PDO index [*Biondi et al.*, 2001] (Figure 3). Annual $\delta^{15}N_{coral}$ record in the 2000s similarly oscillated with the variation of local Kuroshio transport close to Tatsukushi Bay rather than that on 137E line (Figures 2). Previous studies suggested that coral geochemical records (Sr/Ca and $\delta^{18}O_{carbonate}$) in 3 to 5 year running means from north western Pacific are correlated with the PDO index with lags of −2 to +6 years [*Felis et al.*, 2010; *Watanabe et al.*, 2014]. We also applied a 3 year running mean to the all time series to suppress local high-frequency variability in the coral geochemical records and to enhance the common signal between Kuroshio and Pacific climates on interannual to decadal time scales.

The 3 year running mean of the variation of $\delta^{15}N_{coral}$ and the natural logarithm of the Kuroshio transport showed a negative correlation during 1972–2007 (Figures 3 and 4; $R = -0.69$, $P < 0.001$). This result suggests

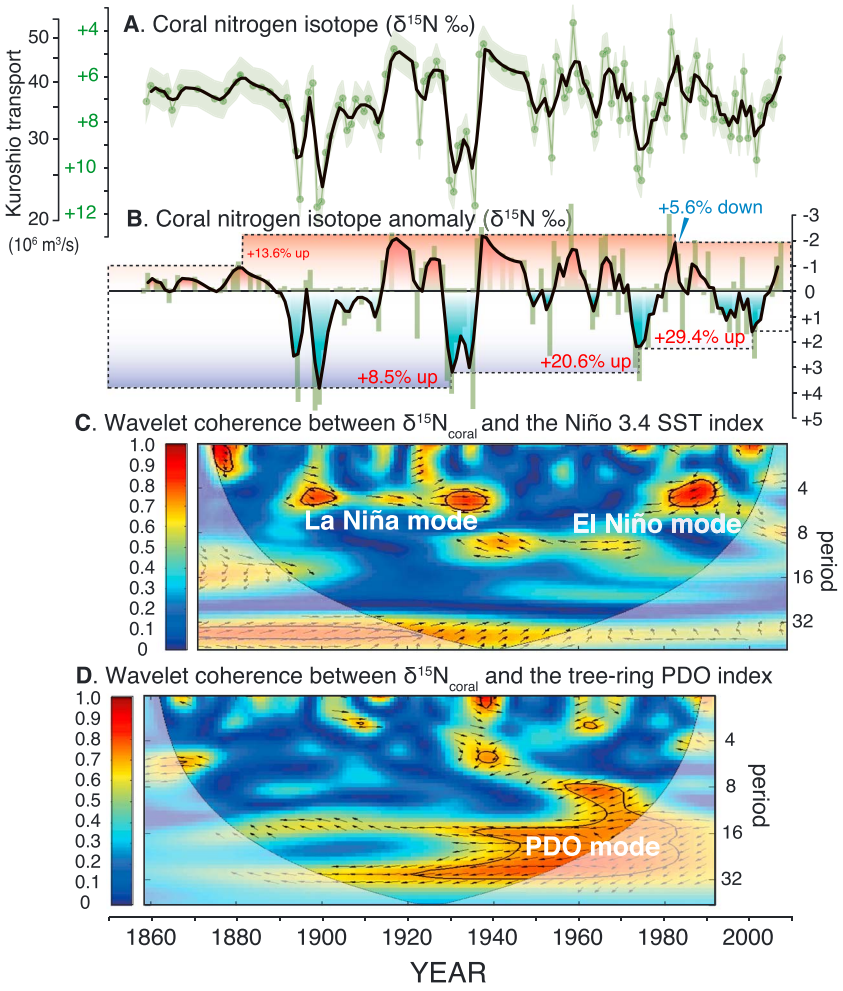

Figure 5. The 150-year record of $\delta^{15}N_{coral}$ compared with the NIÑO3.4 SST index and the PDO index. (a) As the Kuroshio transport proxy, the subannual resolution of the $\delta^{15}N_{coral}$ time series (green) is shown with a 3 year running mean (bold black line). The *y* axis of $\delta^{15}N_{coral}$ is inversed. (b) The anomalies of $\delta^{15}N_{coral}$ (green bars) from the average values of the 150-year $\delta^{15}N_{coral}$ are shown with a 3-year running mean (bold black line). The color shades and the arrows indicate a stronger (red) and weaker (blue) Kuroshio transport. (c) Squared wavelet coherence between $\delta^{15}N_{coral}$ and the NIÑO3.4 SST index (Figure 5c) and between $\delta^{15}N_{coral}$ and the PDO index (Figure 5d). The 5% significance level against red noise is shown as a thick contour on each figure. The relative phase relationship is shown as arrows (with in-phase pointing right, antiphase pointing left, and the climate index leading $\delta^{15}N_{coral}$ by 90° pointing straight down).

that nitrate in the subsurface water of the north Pacific subtropical gyre ($\delta^{15}N_{nitrate}$; +2–+3‰ [*Liu et al.*, 1996; *Casciotti et al.*, 2008]) was supplied by the large transport volume of the Kuroshio Current. The $\delta^{15}N_{coral}$ in the cores from Tatsukushi Bay mainly preserves the variation of the Kuroshio transport that is associated with changes in the isotopic composition of nitrate in surface waters.

$\delta^{15}N_{coral}$ and the proxy of the Kuroshio meander (sea level anomaly on Kushimoto from Uragami, Japan) show no clear correlation (Figure S3), which suggests that the influence of the Kuroshio meander on Tatsukushi Bay is insignificant. The 3-year running mean of $\delta^{15}N_{coral}$ is negatively correlated with that of the PDO index with 2 years of lag (Figure 3; $R = -0.63$, $P < 0.005$) and has similar oscillation in ~7 and ~18-year cycle (Figure S4a). The effect of the intensified Aleutian Low strengthened by a positive PDO would be conveyed to the Kuroshio path through the subtropical gyre 2 years later. Although $\delta^{15}N_{coral}$ shows less correlation with the NIÑO3.4 index, $\delta^{15}N_{coral}$ and the NIÑO3.4 index show a similar oscillation in an ~7-year cycle (Figure S4b), as did the larger Kuroshio transport with the El-Niño state and positive PDO during 1972–1995. Since 1996, the relationship between the $\delta^{15}N_{coral}$-Kuroshio transport and the ENSO-PDO shifted to the opposite, which

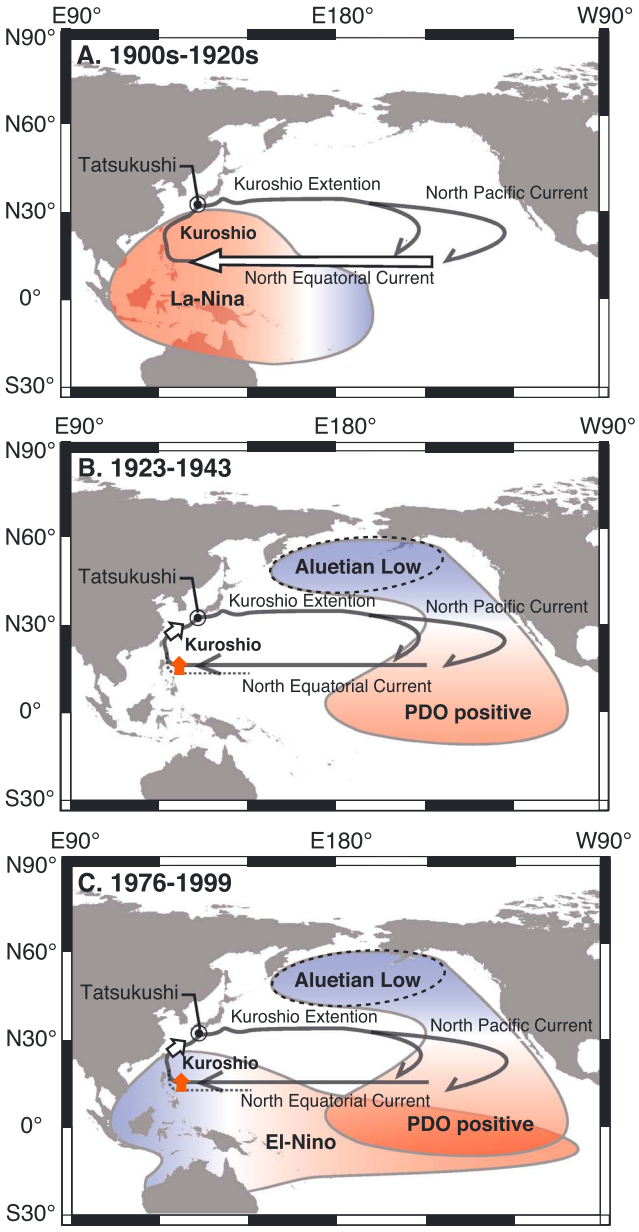

Figure 6. Schematic figures of climatic patterns that increase the Kuroshio transport. (a) The 1900s to 1920s show a La Niña dominant phase, (b) the 1923 to 1943 show a positive PDO dominant phase, and (c) from the 1976 to 1999 shows a combined El Niño and PDO positive phase. The color shades indicate sea surface temperature gradient, warm (red) and cold (blue), in each climate mode. The white arrows indicate intensified currents. The orange arrows indicate northward shifts of the bifurcation latitude of North Equatorial Current.

suggests that the Kuroshio transport has been intensified by the La-Niña state during the most recent 12 years. The linear relationship corresponding to this correlation was used as a proxy for the Kuroshio transport to reconstruct the records of the Kuroshio transport for the past 150 years.

3.3. Reconstructed Kuroshio Transport Throughout the 150 Years

Throughout the 150 years studied, the Kuroshio transport periodically decreased every ~30 years: between 1890 and 1910, in the 1930s, in the late 1970s, and in the early 2000s with the shift in the climate mode controlling the variation in the Kuroshio transport (Figures 5a and 5b). The spectral analysis using the multitaper method confirmed that a 25.6-year cycle is significant in the annual $\delta^{15}N_{coral}$ record (Figure S5). The timing of the decreasing Kuroshio transport in the 1930s and late 1970s corresponded to a simultaneous bidecadal and pentadecadal regime shift weakening the Aleutian Low [*Minobe*, 1999]. These minima of the Kuroshio transport gradually increased by 7%, 15% and 21% compared with the early 1900s (Figure 5b). However, the maxima of the Kuroshio transport increased from $40.6 \times 10^6\ m^3/s$ in the 1880s to $47 \times 10^6\ m^3/s$ in the late 1930s. The maxima of the Kuroshio transport then slightly decreased (by 5.6%) in the early 1980s. The Kuroshio transport was intensified, and its amplitude became smaller. These results suggest that the Kuroshio transport has gradually become stronger and more stable over the past 100 years. Previous climate model studies and reanalyzed observation data also showed the warming and acceleration of the western boundary currents resulting from the intensified wind stress curl from increased atmospheric CO_2 [*Wu et al.*, 2012; *Sakamoto et al.*, 2005; *Saenko et al.*, 2005]. The North Pacific Subtropical Gyre, including the Kuroshio Current, is driven by the westerly jet and trade wind on the ridge of the Hadley cell. The stabilization of the Hadley cell resulting from global warming [*Lu et al.*, 2007] might have stabilized the Kuroshio transport.

3.4. The Relationship Between Kuroshio and ENSO-PDO States

To clarify the relationship between the variation of the Kuroshio transport and the ENSO-PDO state for 150 years (Figure S6), a wavelet coherence analysis [*Grinsted et al.*, 2004] was performed between the annual

$\delta^{15}N_{coral}$ and the annual NIÑO3.4 SST index (Figure 5c) and the annual $\delta^{15}N_{coral}$ and the tree ring PDO index [*Biondi et al.*, 2001] (Figure 5d). In Figure 5c, the positive correlation between $\delta^{15}N_{coral}$ and the NIÑO3.4 SST index are named the La Niña mode, which suggests that the Kuroshio transport increased with a warming state in the western tropical Pacific. The La-Niña mode oscillated on a frequency of 4–7 years between the late 1890s and the late 1930s (Figure 5c). From the late 1930s to the early 1990s, $\delta^{15}N_{coral}$ and the NIÑO3.4 SST index correlated negatively, which we described as the El-Niño mode (Figure 5c). The El Niño mode suggests that the Kuroshio transport increased with a warming state in the eastern tropical Pacific. The El-Niño mode oscillated on ~10-year frequencies, while the El-Niño mode after the 1980s oscillated on a period between 4 and 7 years (Figure 5c). In Figure 5d, $\delta^{15}N_{coral}$ and the tree ring PDO index are negatively correlated through the twentieth century, especially starting in the late 1930s, in period of ~16-year and ~30-year. $\delta^{15}N_{coral}$ variation suggested that the Kuroshio transport increased with both the El-Niño state and the PDO positive mode, but the relationship is rather uncertain before 1930 and might have been opposite. These results suggest that the climate modes that influence the Kuroshio transport have been unstable and have changed over the past 150 years.

The climate modes influencing the variation of the Kuroshio transport appear to have changed during the 20th century (Figure 6). From the 1900s to 1920s, 4–7 year cycles of warming in the western tropical Pacific, known as the La Niña state, increased the Kuroshio transport. Kuroshio current could be intensified due to stronger easterly trade wind on North Equatorial Current in La Niña state (Figure 6a). The Pacific decadal variability is the basis of the ~20 years of variability of the Kuroshio transport since 1940. This decadal change might be generated by the intensity of the winter Aleutian Low [*Trenberth and Hurrell*, 1994], and the effect was conveyed to the Kuroshio path in the northwestern Pacific. In addition to the PDO variability, the El Niño state has also increased the Kuroshio transport since the 1960s (Figures 6b and 6c). The bifurcation latitude of the North Equatorial Current separated into Kuroshio and Mindanao Current shifts northward from Northeast off Philippines to Luzon strait in positive PDO and El Niño state [e.g., *Qiu and Lukas*, 1996; *Qiu and Chen*, 2010; *Hu et al.*, 2015]. As a result, Kuroshio transport is weakened at east of Luzon strait [*Kashino et al.*, 2009] but intensified northeast of Taiwan and downstream [*Wu*, 2013]. Additional work is required to understand the Kuroshio Current system with respect to the interannual to decadal climate variability of the northern Pacific and the future influences of global warming.

Acknowledgments

We thank H. Adachi, M. Ikeda, K. Hyeong, M. Shimamura, T. Yamazaki, K. Nishimoto, S. Nakachi, J. Isasa, and the Tatsukushi Diving Center for their cooperation in the field works. K. Sugihara identified the species of coral specimens. R. Nakaya helped in the subsampling of coral cores. T. Irino supported the oxygen isotope analysis. T. Ohyama performed the water sample analysis. Geological Survey of Hokkaido and T. Nakamura supported the salinity measurements of seawater. The fieldwork was conducted through the financial support of the Environment Research and Technology Development Fund, Ministry of the Environment, Japan (RF-082) and Kuroshio Biological Research Foundation. A. Yamazaki was supported by Grants-in-Aid for JSPS research fellows. $\delta^{15}N_{coral}$ data used in this study are available in Data S1 in the supporting information.

References

Biondi, F., A. Gershunov, and D. R. Cayan (2001), North pacific decadal climate variability since 1661, *J. Clim.*, *14*, 5–10.

Casciotti, K., T. Trull, D. Glover, and D. Davies (2008), Constraints on nitrogen cycling at the subtropical North Pacific Station ALOHA from isotopic measurements of nitrate and particulate nitrogen, *Deep Sea Res., Part II*, *55*(14–15), 1661–1672.

Cobb, K. M., C. D. Charles, H. Cheng, and R. L. Edwards (2003), El Niño/Southern Oscillation and tropical Pacific climate during the last millennium, *Nature*, *424*, 271–276.

D'Asaro, E., C. Lee, L. Rainville, R. Harcourt, and L. Thomas (2011), Enhanced turbulence and energy dissipation at ocean fronts, *Science*, *332*(6027), 318–322.

Earth System Research Laboratory, NOAA (2013), NINO 3.4 SST Index. [Available at http://www.esrl.noaa.gov/psd/data/climateindices/list/.]

Felis, T., A. Suzuki, H. Kuhnert, N. Rimbu, and H. Kawahata (2010), Pacific Decadal Oscillation documented in a coral record of North Pacific winter temperature since 1873, *Geophys. Res. Lett.*, *37*, L14605, doi:10.1029/2010GL043572.

Grinsted, A., J. C. Moore, and S. Jevrejeva (2004), Application of the cross wavelet transform and wavelet coherence to geophysical time series, *Nonlinear Process. Geophys.*, *11*(5/6), 561–566, doi:10.5194/npg-11-561-2004.

Guo, X. Y., X. H. Zhu, Y. Long, and D. J. Huang (2013), Spatial variations in the Kuroshio nutrient transport from the East China Sea to south of Japan, *Biogeosciences*, *10*(10), 6403–6417.

Hanawa, K., and J. Kamada (2001), Variability of core layer temperature (CLT) of the North Pacific subtropical mode water, *Geophys. Res. Lett.*, *28*(11), 2229–2232, doi:10.1029/2000GL011716.

Hirota, A., U. Tsunogai, D. D. Komatsu, and F. Nakagawa (2010), Simultaneous determination of $\delta^{15}N$ and $\delta^{18}O$ of N_2O and $\delta^{13}C$ of CH_4 in nanomolar quantities from a single water sample, *Rapid Commun. Mass Spec.*, *24*(7), 1085–1092.

Hu, D., et al. (2015), Pacific western boundary currents and their roles in climate, *Nature*, *522*(7556), 299–308.

Japan meteorological Agency (2013a), [Available at http://www.data.jma.go.jp/kaiyou/shindan/b_2/kuroshio_flow/kuroshio_flow.html.]

Japan meteorological Agency (2013b), [Available at http://www.data.jma.go.jp/kaiyou/data/shindan/b_2/kuroshio_stream/kuroshio_stream.html.]

Kaneko, H., I. Yasuda, K. Komatsu, and S. Itoh (2012), Observations of the structure of turbulent mixing across the Kuroshio, *Geophys. Res. Lett.*, *39*, L15602, doi:10.1029/2012GL052419.

Kaneko, H., I. Yasuda, K. Komatsu, and S. Itoh (2013), Observations of vertical turbulent nitrate flux across the Kuroshio, *Geophys. Res. Lett.*, *40*, 3123–3127, doi:10.1002/grl.50613.

Kaplan, D., and L. Glass (1995), *Understanding Nonlinear Dynamics*, 420 pp., Springer, New York.

Kashino, Y., N. España, F. Syamsudin, K. Richards, T. Jensen, P. Dutrieux, and A. Ishida (2009), Observations of the North Equatorial Current, Mindanao Current, and Kuroshio current system during the 2006/07 El Niño and 2007/08 La Niña, *J. Oceanogr.*, *65*(3), 325–333.

Knapp, A. N., and D. M. Sigman (2005), N isotopic composition of dissolved organic nitrogen and nitrate at the Bermuda Atlantic Time-series Study site, *Global Biogeochem. Cycles*, *19*, GB1018, doi:10.1029/2004GB002320.

Konno, U., U. Tsunogai, D. D. Komatsu, S. Daita, F. Nakagawa, A. Tsuda, T. Matsui, Y. J. Eum, and K. Suzuki (2010), Determination of total N_2 fixation rates in the ocean taking into account both the particulate and filtrate fractions, *Biogeosciences*, *7*(8), 2369–2377.

Liu, K.-K., M.-J. Su, C.-R. Hsueh, and G.-C. Gong (1996), The nitrogen isotopic composition of nitrate in the Kuroshio Water northeast of Taiwan: Evidence for nitrogen fixation as a source of isotopically light nitrate, *Mar. Chem.*, *54*(3–4), 273–292.

Lu, J., G. A. Vecchi, and T. Reichler (2007), Expansion of the Hadley cell under global warming, *Geophys. Res. Lett.*, *34*, L06805, doi:10.1029/2006GL028443.

Mantua, N. J., S. R. Hare, Y. Zhang, J. M. Wallace, and R. C. Francis (1997), A Pacific interdecadal climate oscillation with impacts on salmon production, *Bull. Am. Meteorol. Soc.*, *78*(6), 1069–1079.

Minobe, S. (1999), Resonance in bidecadal and pentadecadal climate oscillations over the North Pacific: Role in climatic regime shifts, *Geophys. Res. Lett.*, *26*(7), 855–858, doi:10.1029/1999GL900119.

Muscatine, L., C. Goiran, L. Land, J. Jaubert, J. P. Cuif, and D. Allemand (2005), Stable isotopes (^{13}C and ^{15}N) of organic matrix from coral skeleton, *Proc. Natl. Acad. Sci. U.S.A.*, *102*(5), 1525–1530.

Nagai, T., A. Tandon, H. Yamazaki, and M. J. Doubell (2009), Evidence of enhanced turbulent dissipation in the frontogenetic Kuroshio Front thermocline, *Geophys. Res. Lett.*, *36*, L12609, doi:10.1029/2009GL038832.

Nagai, T., A. Tandon, H. Yamazaki, M. J. Doubell, and S. Gallager (2012), Direct observations of microscale turbulence and thermohaline structure in the Kuroshio Front, *J. Geophys. Res.*, *117*, C08013, doi:10.1029/2011JC007228.

Pelegrí, J. L., G. T. Csanady, and A. Martins (1996), The North Atlantic nutrient stream, *J. Oceanogr.*, *52*(3), 275–299.

Qiu, B. (2003), Kuroshio Extension variability and forcing of the Pacific decadal oscillations: Responses and potential feedback, *J. Phys. Oceanogr.*, *33*(12), 2465–2482.

Qiu, B., and S. Chen (2010), Eddy-mean flow interaction in the decadally modulating Kuroshio Extension system, *Deep Sea Res., Part II*, *57*(13–14), 1098–1110.

Qiu, B., and R. Lukas (1996), Seasonal and interannual variability of the North Equatorial Current, the Mindanao Current, and the Kuroshio along the Pacific western boundary, *J. Geophys. Res.*, *101*(C5), 12,315–12,330, doi:10.1029/95JC03204.

Rainville, L., and R. Pinkel (2004), Observations of energetic high-wavenumber internal waves in the Kuroshio, *J. Phys. Oceanogr.*, *34*(7), 1495–1505.

Saenko, O., J. Fyfe, and M. England (2005), On the response of the oceanic wind-driven circulation to atmospheric CO_2 increase, *Clim. Dyn.*, *25*(4), 415–426.

Sakamoto, T. T., H. Hasumi, M. Ishii, S. Emori, T. Suzuki, T. Nishimura, and A. Sumi (2005), Responses of the Kuroshio and the Kuroshio Extension to global warming in a high-resolution climate model, *Geophys. Res. Lett.*, *32*, L14617, doi:10.1029/2005GL023384.

Sawada, K., and N. Handa (1998), Variability of the path of the Kuroshio ocean current over the past 25,000 years, *Nature*, *392*(6676), 592–595.

Trenberth, K., and J. Hurrell (1994), Decadal atmosphere-ocean variations in the Pacific, *Clim. Dyn.*, *9*(6), 303–319.

Tsunogai, U., T. Kido, A. Hirota, S. B. Ohkubo, D. D. Komatsu, and F. Nakagawa (2008), Sensitive determinations of stable nitrogen isotopic composition of organic nitrogen through chemical conversion into N_2O, *Rapid Commun. Mass Spec.*, *22*(3), 345–354.

Tsunogai, U., D. D. Komatsu, S. Daita, G. A. Kazemi, F. Nakagawa, I. Noguchi, and J. Zhang (2010), Tracing the fate of atmospheric nitrate deposited onto a forest ecosystem in Eastern Asia using $\Delta^{17}O$, *Atmos. Chem. Phys.*, *10*(4), 1809–1820.

Ujiié, Y., H. Ujiié, A. Taira, T. Nakamura, and K. Oguri (2003), Spatial and temporal variability of surface water in the Kuroshio source region, Pacific Ocean, over the past 21,000 years: Evidence from planktonic foraminifera, *Mar. Micropaleontol.*, *49*(4), 335–364.

Watanabe, T., et al. (2011), Permanent El Niño during the Pliocene warm period not supported by coral evidence, *Nature*, *471*(7337), 209–211.

Watanabe, T., T. Kawamura, A. Yamazaki, M. Murayama, and H. Yamano (2014), A 106 year monthly coral record reveals that the East Asian summer monsoon modulates winter PDO variability, *Geophys. Res. Lett.*, *41*, 3609–3614, doi:10.1002/2014GL060037.

Wu, C.-R. (2013), Interannual modulation of the Pacific Decadal Oscillation (PDO) on the low-latitude western North Pacific, *Prog. Oceanogr.*, *110*, 49–58.

Wu, Y. J., et al. (2012), Occurrence of elves and lightning during El Niño and La Niña, *Geophys. Res. Lett.*, *39*, L03106, doi:10.1029/2011GL049831.

Yamagata, T., Y. Shibao, and S.-i. Umatanit (1985), Interannual variability of the Kuroshio Extension and its relation to the Southern Oscillation/El Niño, *J. Oceanogr. Soc. Jpn.*, *41*(4), 274–281.

Yamazaki, A., T. Watanabe, K. Sowa, S. Nakachi, H. Yamano, and F. Iwase (2009), Reconstructing palaeoenvironments of temperate regions based on high latitude corals at Tatsukushi Bay in Japan, *J. Jpn. Coral Reef Soc.*, *11*(1), 91–107.

Yamazaki, A., T. Watanabe, N. O. Ogawa, N. Ohkouchi, K. Shirai, M. Toratani, and M. Uematsu (2011), Seasonal variations in the nitrogen isotope composition of Okinotori coral in the tropical western Pacific: A new proxy for marine nitrate dynamics, *J. Geophys. Res.*, *116*, G04005, doi:10.1029/2011JG001697.

Yamazaki, A., T. Watanabe, N. Takahata, Y. Sano, and U. Tsunogai (2013), Nitrogen isotopes in intra-crystal coralline aragonites, *Chem. Geol.*, *351*, 276–280.